

Height fluctuations in the honeycomb dimer model

Richard Kenyon *

Abstract

We study a model of random crystalline surfaces arising in the dimer model on the honeycomb lattice. For a fixed “wire frame” boundary condition, as the lattice spacing $\epsilon \rightarrow 0$, Cohn, Kenyon and Propp [3] showed the almost sure convergence of a random surface to a non-random limit shape Σ_0 . We show here that when Σ_0 has no facets, for a large family of boundary conditions approximating the wire frame, the large-scale surface fluctuations (height fluctuations) about Σ_0 converge as $\epsilon \rightarrow 0$ to a Gaussian free field for an appropriate conformal structure determined by Σ_0 . We also show that the local statistics of the fluctuations near a given point x are given by the unique ergodic Gibbs measure (on plane configurations) whose slope is the slope of the tangent plane of Σ_0 at x .

1 Introduction

1.1 Dimers and surfaces

A **dimer covering**, or *perfect matching*, of a graph is a set of edges covering all the vertices exactly once. In this paper we study the dimer model on the **honeycomb lattice** (the periodic planar graph whose faces are regular hexagons). This model, and more generally dimer models on other periodic bipartite planar graphs, are statistical mechanical models for discrete random interfaces. Part of their interest lies in the conformal invariance properties of their scaling limits [6, 7].

Dimer coverings of the honeycomb graph are dual to tilings with 60° rhombi, also known as **lozenges**, see Figure 1. Lozenge tilings can in turn be viewed as orthogonal projections onto the plane $P_{111} = \{x + y + z = 0\}$ of **stepped surfaces** which are polygonal surfaces in \mathbb{R}^3 whose faces are squares in the 2-skeleton of \mathbb{Z}^3 (the stepped surfaces are *monotone* in the sense that the projection is injective), see Figures 1,2. Each stepped surface is the graph of a function, the **normalized height function**, on the underlying tiling, which is linear on each tile.

*Laboratoire de Mathématiques UMR 8628 du CNRS, Bât 425, Université Paris-Sud, 91405 Orsay, France.

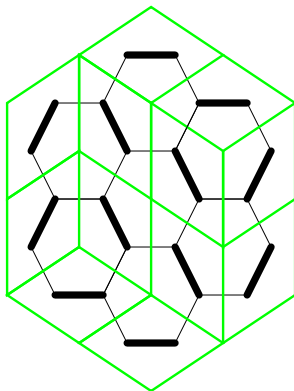


Figure 1: Honeycomb dimers (solid) and the corresponding “lozenge” tilings (gray/green).

1.2 Scaling limit

We are interested in studying the **scaling limit** of the honeycomb dimer model, that is, the limiting behavior of a uniform random dimer covering of a fixed plane region when the lattice spacing ϵ goes to zero; correspondingly, the stepped surfaces are surfaces in $\epsilon\mathbb{Z}^3$. As boundary conditions we are interested the scaling limit of a stepped surface spanning a wire frame γ_ϵ in $\epsilon\mathbb{Z}^3$ which is converging to a fixed smooth wire frame γ as $\epsilon \rightarrow 0$.

Let γ be a smooth closed curve in \mathbb{R}^3 which can be spanned by a smooth simply-connected surface Σ whose normal ν points into the positive orthant $\mathbb{R}_{>0}^3$, and such that the orthogonal projection of Σ to the plane $P_{111} = \{(x, y, z) \mid x + y + z = 0\}$ is injective. Let U be the projection of Σ .

For each $\epsilon > 0$ let γ_ϵ be a nearest-neighbor path in $\epsilon\mathbb{Z}^3$ approximating γ , and which can be spanned by a monotone stepped surface Σ_ϵ , monotone in the sense that orthogonal projection $\pi_{111}(\Sigma_\epsilon)$ of Σ_ϵ to the plane P_{111} is injective. See for example Figure 2 (although there the boundary is only piecewise smooth).

For a given γ_ϵ there are many spanning surfaces Σ_ϵ and we study the limiting properties of the uniform measure on the set of Σ_ϵ as $\epsilon \rightarrow 0$.

1.3 Statement

In [3] it was shown that, for a uniform random surface Σ_ϵ spanning γ_ϵ , the distribution of the normalized height function h_ϵ (defined on $U_\epsilon = \pi_{111}(\gamma_\epsilon)$ and whose graph is Σ_ϵ) converges as $\epsilon \rightarrow 0$ to a *nonrandom* function \bar{h} , the **asymptotic height function** on U , whose graph is a smooth surface Σ_0 spanning γ . The limiting surface Σ_0 minimizes a certain surface energy functional arising from purely combinatorial considerations: the “energy” is the negative of the exponential growth rate of the number of discrete surfaces Σ_ϵ lying near Σ_0 .

In this paper we show that, if the precise local behavior of the approximating curves γ_ϵ is chosen in a particular way, then both the local statistics and the global height

fluctuations of Σ_ϵ can be determined. We show that the local statistics of Σ_ϵ near a given point are given by the unique Gibbs measure of slope equal to the slope of \bar{h} at that point (see Theorem 2.1 and Theorem 6.1), and the fluctuations of the *unnormalized* height function, $\frac{1}{\epsilon}(h_\epsilon - \bar{h})$, have a weak limit as $\epsilon \rightarrow 0$ which is the pull-back of the **Gaussian free field** on the unit disk \mathbb{D} (see below) under a particular diffeomorphism $\phi : U \rightarrow \mathbb{D}$. For the exact statement see Theorem 7.1. One proviso is that we do not consider the cases in which \bar{h} has **facets**, that is, for our results we require that the normal to the graph of \bar{h} be *strictly* inside the positive orthant (whereas the results of [3] do not require this restriction). This is a shortcoming only of our techniques; we believe that the result holds in greater generality.

This work builds on work of [7, 5]. Previously Theorem 7.1 was proved for a different dimer model (dimers on \mathbb{Z}^2) in a special case which in our context corresponds to the wire frame γ lying in the plane P_{111} , see [7]. In that case the conformal structure is the standard conformal structure on U : ϕ is a conformal diffeomorphism. The corresponding result with periodic boundary conditions (and with constant, nonzero slope) was done in [5].

In the present case we still require special boundary conditions, which generalize the ‘‘Temperlian’’ boundary conditions of [6, 7]. It remains an open question whether the result holds for all boundary conditions.

1.4 Gaussian free field

The Gaussian free field on \mathbb{D} [14] is a Gaussian process which is a conformally invariant, two-dimensional cousin of Brownian motion (or more precisely, of the Brownian bridge). It is the simplest example of a random conformal field. It is best thought of as a random (signed) measure. Integrated against any smooth test function ψ on \mathbb{D} it yields a Gaussian real variable of mean zero and variance given by

$$\int_{\mathbb{D}} \int_{\mathbb{D}} \psi(x_1) \psi(x_2) G(x_1, x_2) |dx_1|^2 |dx_2|^2,$$

where the kernel G is the Dirichlet Green’s function on \mathbb{D} . This statement can in fact be taken as the definition of the Gaussian free field.

1.5 Beltrami coefficient

Since the Gaussian free field is invariant under conformal mappings, our theorem can be restated as saying that the fluctuations of Σ_ϵ are given by the Gaussian free field for a particular conformal structure on U . A conformal structure on U can be described by a Beltrami differential $\mu(z) \frac{d\bar{z}}{dz}$. That is, if $\phi : U \rightarrow \mathbb{D}$ is a diffeomorphism then

$$\mu(z) \frac{d\bar{z}}{dz} = \frac{\phi_{\bar{z}} d\bar{z}}{\phi_z dz}$$

is invariant under post-composition of ϕ with a conformal map. In the current case the relevant conformal structure is a simple function of the normal (p_a, p_b, p_c) to the

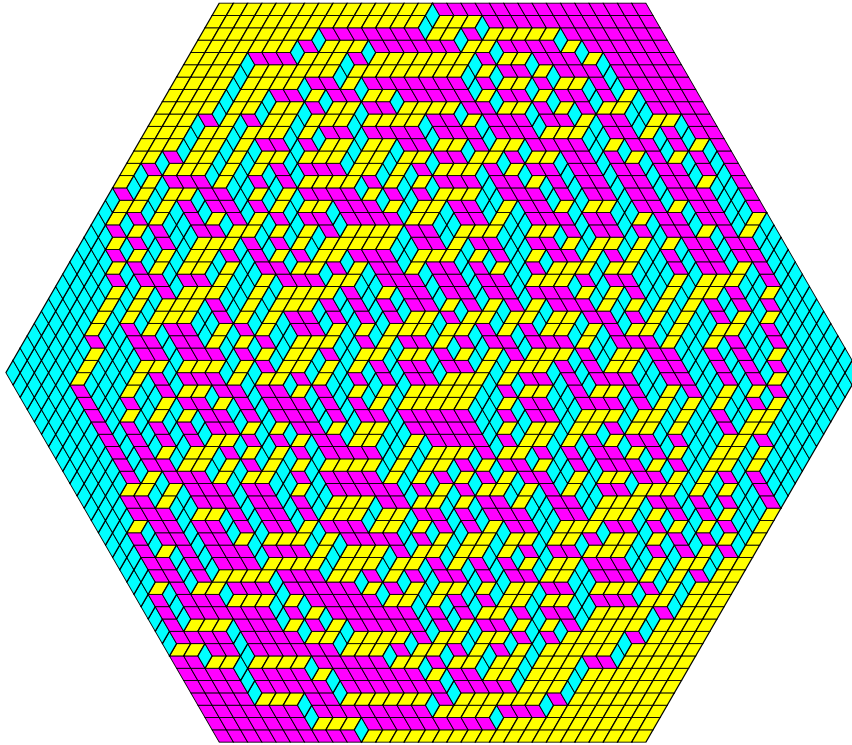


Figure 2: Boxed plane partition.

graph of \bar{h} (which we scale so that $p_a + p_b + p_c = 1$). For example if the wire frame γ is contained in a plane, the conformal structure is a linear image of the standard conformal structure. The Beltrami coefficient of the linear mapping ϕ is a constant

$$\mu(z) = \frac{\phi_{\bar{z}}}{\phi_z} = \frac{ce^{i\pi p_b} - ae^{\pi i/3}}{ce^{i\pi p_b} - ae^{-i\pi/3}}$$

where $a = \sin(\pi p_a)$ and $c = \sin(\pi p_c)$. In geometric terms ϕ is an \mathbb{R} -linear mapping of \mathbb{C} which takes the equilateral triangle $\{0, 1, e^{\pi i/3}\}$ to the triangle with angles $(\pi p_a, \pi p_b, \pi p_c)$, taking 0 to the vertex with angle πp_b .

For general \bar{h} , $\mu(z)$ has the above form where p_a, p_b, p_c are functions of z .

1.6 Example

Consider the **boxed plane partition** (BPP) (Figure 2), which is a random lozenge tiling of a regular hexagon. In [4] it was shown that, for a random tiling of the hexagon, the asymptotic height function \bar{h} is linear outside of the inscribed circle and analytic inside (with an explicit but complicated formula). Although our theorem does not apply to this case because of the “frozen” regions, or facets, outside the inscribed circle, if we choose boundary conditions inside the inscribed circle, our results apply. Suppose

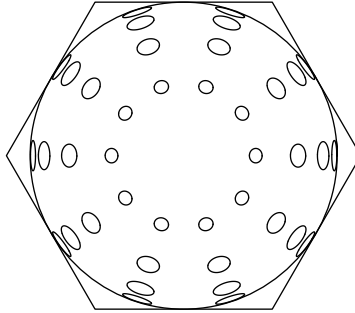


Figure 3: The ellipse field associated to the Beltrami coefficient inside the BPP is rotationally symmetric.

that the hexagon has sides of length 1, so that the inscribed circle has radius $\sqrt{3}/2$. Let U be a disk of radius $r < \sqrt{3}/2$ concentric with it. Suppose that the normalized height function on the boundary of U is chosen to agree with the asymptotic height function of corresponding region in the BPP, so that the asymptotic height function of U equals the asymptotic height function of the BPP restricted to U . Then the fluctuations on U can be computed explicitly: take the standard conformal structure on a hemisphere in \mathbb{R}^3 , and project it orthogonally onto the plane containing its equator. Identifying the equator with the inscribed circle in the BPP gives the relevant conformal structure in U . Remarkably, in this example the Beltrami coefficient is rotationally invariant, even though \bar{h} itself is not. See Figure 3 and section 8. We conjecture that the fluctuations for the BPP are given by the limit $r \rightarrow \sqrt{3}/2$ of this construction (it is known [4] that fluctuations in the “frozen” regions outside the circle are exponentially small in $1/\epsilon$).

1.7 Proof outline

The main goal is to compute the asymptotic expansion of the inverse Kasteleyn matrix. This is complicated by the fact that it grows exponentially when the boundary height function is not horizontal. However by pre- and post-composition with an appropriate diagonal matrix, we can remove the exponential growth and relate K^{-1} to the Green’s function with Dirichlet boundary conditions on another graph.

Here is a sketch of the main ideas.

1. For each ϵ we define a directed graph \mathcal{G}_T embedded in the upper half plane \mathbb{H} , and a geometric map ϕ from U_ϵ to \mathcal{G}_T , such that the spanning tree model on \mathcal{G}_T is in isomorphism (via the construction of [11]) with the dimer model on U_ϵ . The existence of such a graph \mathcal{G}_T follows in a large part from [11] and [12].
2. The Kasteleyn matrix K on U_ϵ is related to the discrete Laplacian on \mathcal{G}_T after a “gauge transformation”, which consists of pre- and post-composing K by an (exponentially growing) diagonal matrix.
3. Standard techniques for discrete harmonic functions yield an asymptotic expan-

sion for the Green's function on \mathcal{G}_T .

4. The asymptotic expansion of the coupling function (inverse Kasteleyn matrix) on U_ϵ is obtained from the derivative of the Green's function on \mathcal{G}_T , pulled back under the mapping ϕ .
5. Asymptotic expansions of the moments of the height fluctuations are computed via integrals of the asymptotic coupling function. These moments are the moments of the Gaussian free field on \mathbb{H} pulled back under ϕ .

Acknowledgments. Many ideas in this paper were inspired by conversations with Henry Cohn, Jim Propp, Jean-René Geoffroy, Scott Sheffield, Béatrice deTilière, Cédric Boutillier, and Andrei Okounkov. This paper was completed while the author was visiting Princeton University.

2 Definitions

2.1 Graphs

Let π_{111} be the orthogonal projection of \mathbb{R}^3 onto P_{111} . Let e_1, e_2, e_3 be the π_{111} -projections of the unit basis vectors, and $\hat{x} = e_1 - e_2, \hat{y} = e_2 - e_3, \hat{z} = e_3 - e_1$. Let \mathcal{H} be the honeycomb lattice in \mathbb{R}^2 : vertices of \mathcal{H} are $L \cup (L + e_1)$, where L is the lattice $L = \mathbb{Z}(e_1 - e_2) + \mathbb{Z}(e_2 - e_3) = \mathbb{Z}\hat{x} + \mathbb{Z}\hat{y}$, and edges connect nearest neighbors. Vertices in L are colored white, those in $L + e_1$ are black. See Figure 4.

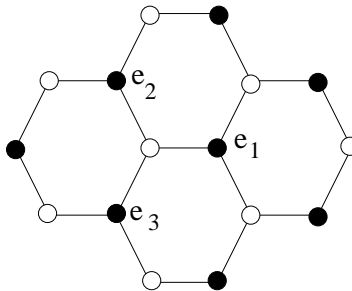


Figure 4: The honeycomb graph.

Let U be a smooth Jordan domain in P_{111} . Let \mathcal{G} be the subgraph of $\epsilon\mathcal{H}$ bounded by a simple closed polygonal path in $\epsilon\mathcal{H}$, approximating ∂U . We assume that \mathcal{G} has a perfect matching. In section 4.3 we will construct from \mathcal{G} a graph \mathcal{G}_D with slightly different boundary conditions.

We define a special kind of dual graph \mathcal{G}^* as follows. Let \mathcal{H}^* be the usual planar dual of \mathcal{H} . For each white vertex of \mathcal{G} take the corresponding triangular face of \mathcal{H}^* ; the union of the edges forming these triangles, along with the corresponding vertices, forms \mathcal{G}^* . In other words, \mathcal{G}^* has a face for each white vertex of \mathcal{G} , as well as for black vertices which have all three neighbors in \mathcal{G} . See Figure 5.

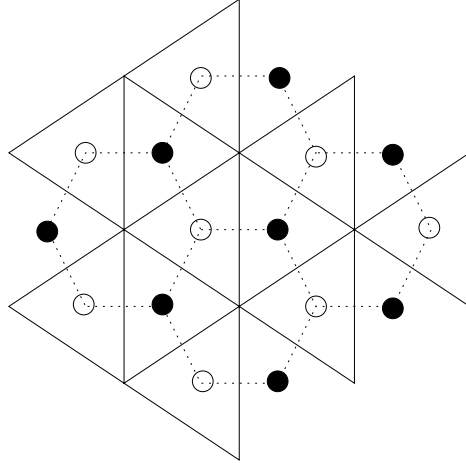


Figure 5: The “dual” graph (solid lines) of the graph of Figure 4.

For an edge in \mathcal{G} , joining vertices b and w , we denote by $(bw)^*$ the dual edge in \mathcal{G}^* (directed at $+90^\circ$ from bw).

2.2 Heights and asymptotics

The **unnormalized** height function, or just height function, of a tiling is the integer-valued function on the vertices of the lozenges (faces of \mathcal{G}) which is the sum of the coordinates of the corresponding point in \mathbb{Z}^3 . It changes by ± 1 along each edge of a tile. The normalized height function is $\epsilon/\sqrt{2}$ times the height function, and is the function whose graph is the surface in $\epsilon\mathbb{Z}^3$.

Let $u : \partial U \rightarrow \mathbb{R}$ be a continuous function with the property that u can be extended to a smooth function \tilde{u} on the interior of U having the property that the normal to the graph of \tilde{u} has nonnegative coordinates, that is, the normal points into the positive orthant $\mathbb{R}_{\geq 0}^3$.

Under these conditions [3] proved the existence of an **asymptotic height function** $\bar{h} : U \rightarrow \mathbb{R}$ (whose graph also has normal with nonnegative coordinates) with boundary values u , which is the asymptotic value of the normalized height function of a uniformly chosen lozenge tiling of any tilable polygon approximating U , whose normalized boundary height function approximates u .

Let $\nu = (p_a, p_b, p_c)$ be the normal vector to the graph of \bar{h} , scaled so that $p_a + p_b + p_c = 1$. By hypothesis $p_a, p_b, p_c \geq 0$; however **we assume that** $p_a, p_b, p_c > \eta > 0$

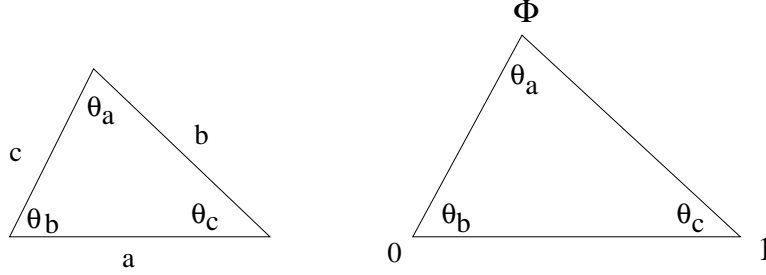


Figure 6: The triangle and a scaled copy with vertices $0, 1, \Phi$.

throughout U for some fixed η . We have

$$\begin{aligned}
 \sqrt{2} \frac{\partial \bar{h}}{\partial \bar{y}} &= 3p_a - 1 \\
 \sqrt{2} \frac{\partial \bar{h}}{\partial \bar{z}} &= 3p_b - 1 \\
 \sqrt{2} \frac{\partial \bar{h}}{\partial \bar{x}} &= 3p_c - 1.
 \end{aligned} \tag{1}$$

Let $\theta_a = \pi p_a, \theta_b = \pi p_b, \theta_c = \pi p_c$. Let a, b, c be the edges of a Euclidean triangle with angles $\theta_a, \theta_b, \theta_c$. Let $z = -e^{-i\theta_c}$ and $w = -e^{i\theta_b}$ so that $a + bz + cw = 0$. See Figure 6. All of these quantities are functions on U , although a, b, c are only defined up to scale.

2.3 Measures and gauge equivalence

We let $\mu = \mu(\mathcal{G})$ be the uniform measure on dimer configurations on a finite graph \mathcal{G} .

If edges of \mathcal{G} are given positive real weights, we can define a new probability measure, the **Boltzmann measure**, giving a configuration a probability proportional to the product of its edge weights.

Certain edge-weight functions lead to the same Boltzmann measure: in particular if we multiply by a constant the weights of all the edges in \mathcal{G} having a fixed vertex, the Boltzmann measure does not change, since exactly one of these weights is used in every configuration. More generally, two weight functions ν_1, ν_2 are said to be **gauge equivalent** if ν_1/ν_2 is a product of such operations, that is, if there are functions F_1 on white vertices and F_2 on black vertices so that for each edge wb , $\nu_1(wb)/\nu_2(wb) = F_1(w)F_2(b)$. Gauge equivalent weights define the same Boltzmann measure.

For planar graphs, two edge-weight functions are gauge equivalent if and only if they have the same **face weights**, where the weight of a face is defined to be the alternating product of the edge weights around the face (that is, the first, divided by the second, times the third, and so on) [10].

In this paper we will only consider weights which are gauge equivalent to constant weights (or nearly so), so the Boltzmann measure will always be the uniform measure.

2.4 Measures in infinite volume

On the infinite honeycomb graph \mathcal{H} there is a two-parameter family of natural translation-invariant and ergodic probability measures on dimer configurations, which restrict to the uniform measure on finite regions (when conditioned on the complement of the finite region), that is, they are **conditionally uniform**. Such measures are also known as **Gibbs measures**. They are classified in the following theorem due to Sheffield.

Theorem 2.1 ([15]) *For each $\nu = (p_a, p_b, p_c)$ with $p_a, p_b, p_c \geq 0$ and scaled so that $p_a + p_b + p_c = 1$ there is a unique translation-invariant ergodic Gibbs measure $\mu = \mu_\nu$ on dimer coverings of \mathcal{H} whose height function has average normal ν . It can be obtained as the limit as $n \rightarrow \infty$ of the uniform measure on tilings of $\mathcal{H}_n = \mathcal{H}/nL$ conditioned on having average normal tending to ν . Moreover every ergodic Gibbs measure is of the above type for some ν .*

Associated to μ_ν is an infinite matrix, the **inverse Kasteleyn matrix** or coupling function, $K_\nu^{-1} = (K_\nu^{-1}(\mathbf{b}, \mathbf{w}))$ whose rows index the black vertices and columns index the white vertices, and whose minors give local statistics for μ_ν . From the method of [10] there is an explicit formula for K_ν^{-1} : if $\mathbf{w} = m_1\hat{x} + n_1\hat{y}$ and $\mathbf{b} = e_1 + m_2\hat{x} + n_2\hat{y} = \mathbf{w} + e_1 + m\hat{x} + n\hat{y}$ then

$$K_\nu^{-1}(\mathbf{b}, \mathbf{w}) = a\left(\frac{a}{b}\right)^m \left(\frac{b}{c}\right)^n K_{abc}^{-1}(\mathbf{b}, \mathbf{w}),$$

where a, b, c are as defined in the previous section and

$$\begin{aligned} K_{abc}^{-1}(\mathbf{b}, \mathbf{w}) &= \frac{1}{(2\pi i)^2} \int_{\mathbb{T}^2} \frac{z_1^{-m+n} w_1^{-n}}{a + bz_1 + cw_1} \frac{dz_1}{z_1} \frac{dw_1}{w_1} \\ &= \frac{1}{\pi} \operatorname{Im} \left(\frac{z^{-m+n} w^{-n}}{cwm + an} \right) + O\left(\frac{1}{m^2 + n^2}\right). \end{aligned}$$

Defining $F(\mathbf{w}) = (bz/a)^{m_1} (cw/bz)^{n_1}$ and $F(\mathbf{b}) = a(bz/a)^{-m_2} (cw/bz)^{-n_2}$ we have

$$K_\nu^{-1}(\mathbf{b}, \mathbf{w}) = \frac{1}{\pi} \operatorname{Im} \left(\frac{F(\mathbf{w})F(\mathbf{b})}{cwm + an} \right) + |F(\mathbf{b})F(\mathbf{w})| O\left(\frac{1}{m^2 + n^2}\right). \quad (2)$$

We'll use this function F below.

2.5 T -graphs

2.5.1 Definition

T -graphs were defined and studied in [12]. A pairwise disjoint collection L_1, L_2, \dots, L_n of open line segments in \mathbb{R}^2 **forms a T -graph in \mathbb{R}^2** if $\cup_{i=1}^n L_i$ is connected and contains all of its limit points except for some finite set $R = \{r_1, \dots, r_m\}$, where each r_i lies on the boundary of the infinite component of \mathbb{R}^2 minus the closure of $\cup_{i=1}^n L_i$. See Figure 7 for an example where the outer boundary is a polygon. Elements in R are called **root vertices**; the L_i are called **complete edges**. We only consider the case

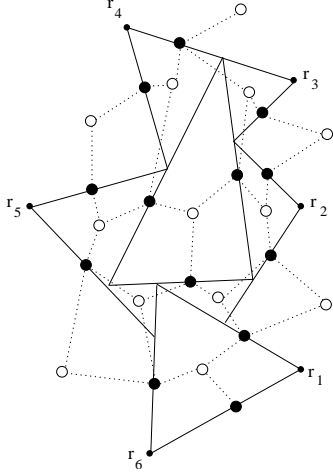


Figure 7: A T -graph (solid) and associated graph \mathcal{G}_D (dotted).

that the outer boundary of the T -graph is a simple polygon, and the root vertices are the convex vertices of this polygon.

Associated to a T -graph is a Markov chain \mathcal{G}_T , whose vertices are the points which are endpoints of some L_i . Each non-root vertex is in the interior of a unique L_j (because the L_j are disjoint); there is a transition from that vertex to its adjacent vertices along L_j , and the transition probabilities are proportional to the inverses of the Euclidean distances. Root vertices are sinks of the Markov chain.

Note that the coordinate functions are harmonic functions on $\mathcal{G}_T \setminus R$. More generally, any function f on \mathcal{G}_T which is harmonic on $\mathcal{G}_T \setminus R$ (we refer to such functions as harmonic functions on \mathcal{G}_T) has the property that it is linear along edges, that is, if v_1, v_2, v_3 are vertices on the same complete edge then

$$\frac{f(v_1) - f(v_2)}{v_1 - v_2} = \frac{f(v_2) - f(v_3)}{v_2 - v_3}.$$

2.5.2 Associated dimer graph and Kasteleyn matrix

Associated to a T -graph is a weighted bipartite planar graph \mathcal{G}_D constructed as follows. Black vertices of \mathcal{G}_D are the L_j . White vertices are the bounded complementary regions, as well as one white vertex for each boundary path joining consecutive root vertices r_j and r_{j+1} (but not for the path from r_m to r_1). The complementary regions are called **faces**; the paths between adjacent root vertices are called **outer faces**. Edges connect the L_i to each face it borders along a positive-length subsegment. The edge weights are equal to the Euclidean length of the bounding segment.

To \mathcal{G}_D there is a canonically associated **Kasteleyn matrix** of \mathcal{G}_D : this is the $n \times n$ matrix $K_{\mathcal{G}_D} = (K_{\mathcal{G}_D}(\mathbf{w}, \mathbf{b}))$ with rows indexing the white vertices and columns indexing the black vertices of \mathcal{G}_D . We have $K_{\mathcal{G}_D}(\mathbf{w}, \mathbf{b}) = 0$ if \mathbf{w} and \mathbf{b} are not adjacent, and otherwise $K_{\mathcal{G}_D}(\mathbf{w}, \mathbf{b})$ is the complex number equal to the edge vector corresponding to

the edge of the region w along complete edge b (taken in the cclw direction around w). In particular $|K_{\mathcal{G}_D}(w, b)|$ is the length of the corresponding edge of w .

Lemma 2.2 $K_{\mathcal{G}_D}$ is a Kasteleyn matrix for \mathcal{G}_D , that is, the alternating product of the matrix entries for edges around a bounded face is positive real or negative real according to whether the face has $2 \bmod 4$ or $0 \bmod 4$ edges, respectively.

By alternating product we mean the first, divided by the second, times the third, etc.

Proof: Let f be a bounded face of \mathcal{G}_D (we mean not one of the outer faces). It corresponds to a meeting point of two or more complete edges; this meeting point is in the interior of exactly one of these complete edges. See Figure 8. In \mathcal{G}_D , for each other black vertex on that face the two edges of the T -graph to neighboring white vertices have opposite orientations. This implies the result. \square

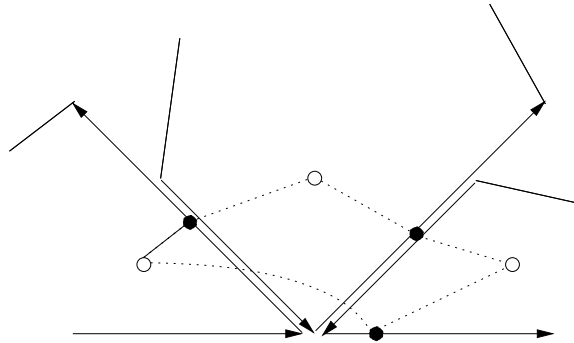


Figure 8: A face of \mathcal{G}_D (dotted).

In [12] it is shown that in-directed spanning forests of \mathcal{G}_T (rooted at the root vertices and weighted by the product of the transition probabilities) are in measure-preserving bijection with dimer coverings of \mathcal{G}_D .

2.5.3 Harmonic functions and discrete analytic functions

To a harmonic function f on a T -graph \mathcal{G}_T we associate a derivative df which is a function on black vertices of \mathcal{G}_D satisfying, for every interior white vertex w ,

$$\sum_{b \in B} K_{\mathcal{G}_D}(w, b) df(b) = 0,$$

as follows (such functions are called **discrete analytic functions** [8]). Let v_1 and v_2 be two distinct points on complete edge b , considered as complex numbers. We define

$$df(b) = \frac{f(v_2) - f(v_1)}{v_2 - v_1}. \quad (3)$$

Since f is linear along any complete edge, df is independent of the choice of v_1 and v_2 .

Lemma 2.3 *With the above definition $\sum_{\mathbf{b} \in B} K_{\mathcal{G}_D}(\mathbf{w}, \mathbf{b}) df(\mathbf{b}) = 0$ for any interior white vertex \mathbf{w} .*

Proof: Let $\mathbf{b}_1, \dots, \mathbf{b}_k$ be the neighbors of \mathbf{w} in cyclic order. To each neighbor \mathbf{b}_i is associated a segment of a complete edge L_i . Let v_i and v_{i+1} be the endpoints of that segment, and w_i and w'_i be the endpoints of L_i . Then

$$\frac{f(v_{i+1}) - f(v_i)}{v_{i+1} - v_i} = \frac{f(w'_i) - f(w_i)}{w'_i - w_i}$$

since the harmonic function is linear along L_i . In particular

$$K_{\mathcal{G}_D}(\mathbf{w}, \mathbf{b}_i) df(\mathbf{b}_i) = (v_{i+1} - v_i) \frac{f(w'_i) - f(w_i)}{w'_i - w_i} = f(v_{i+1}) - f(v_i).$$

Summing over i (with cyclic indices) yields the result. \square

Note that at a boundary white vertex \mathbf{w} , $\sum_B K_{\mathcal{G}_D}(\mathbf{w}, \mathbf{b}) df(\mathbf{b})$ is the difference in f -values at the adjacent root vertices of \mathcal{G}_T .

The construction in the above lemma can be reversed, starting from a discrete analytic function df (on black vertices of \mathcal{G}_D) and integrating to get a harmonic function f on \mathcal{G}_T : define f arbitrarily at a vertex of \mathcal{G}_T and then extend to neighboring vertices (on a same complete edge) using (3). The extension is well-defined by discrete analyticity.

2.5.4 Green's function and $K_{\mathcal{G}_D}^{-1}$

We can relate $K_{\mathcal{G}_D}^{-1}$ to the conjugate Green's function on \mathcal{G}_T using the construction of the previous section, as follows. Let \mathbf{w} be an interior face of \mathcal{G}_T , and ℓ a path from a point in \mathbf{w} to the outer boundary of \mathcal{G}_T which misses all the vertices of \mathcal{G}_T . For vertices v of \mathcal{G}_T , define the **conjugate Green's function** $G^*(\mathbf{w}, v)$ to be the expected algebraic number of crossings of ℓ by the simple random walk started at v and stopped at the boundary. This is the unique function with zero boundary values which is harmonic everywhere except for a jump discontinuity of -1 across ℓ when going cclw around \mathbf{w} . (If there were two such functions, their difference would be harmonic everywhere with zero boundary values.)

Let $K_{\mathcal{G}_D}^{-1}(\mathbf{b}, \mathbf{w})$ be the discrete analytic function of \mathbf{b} defined from $G^*(\mathbf{w}, v)$ as in the previous section; on an edge which crosses ℓ , define $K_{\mathcal{G}_D}^{-1}(\mathbf{b}, \mathbf{w})$ using two points on \mathbf{b} on the same side of ℓ . This function clearly satisfies $K_{\mathcal{G}_D} K_{\mathcal{G}_D}^{-1} = I$ (and in particular is independent of the choice of ℓ).

Note that $K_{\mathcal{G}_D}^{-1}$ also has a probabilistic interpretation: take two particles, started simultaneously at two different points v_1, v_2 of the same complete edge, and couple their random walks so that they start independently and when they meet they stick together for all future times. Then the difference in their winding numbers around \mathbf{w} is determined by their crossings of ℓ before they meet. That is, $K_{\mathcal{G}_D}^{-1}(\mathbf{b}, \mathbf{w})(v_1 - v_2)$ is the expected difference in crossings before the particles meet or until they hit the boundary, whichever comes first.

3 Constant-slope case

3.1 T -graph construction

In this section we compute the asymptotic expansion of $K_{\mathcal{G}_D}^{-1}$ (Theorem 3.5) in the special case is when γ is planar, that is, the normalized asymptotic height function \bar{h} is linear. This case already contains most of the complexity of the general case, which is treated in section 4.

Let $\nu = (p_a, p_b, p_c)$ be the normal to \bar{h} . The angles $\theta_a, \theta_b, \theta_c$ are constant, and we choose a, b, c as before to be constant as well. Define a function $F(\mathbf{w}) = (bz/a)^m (cw/bz)^n$ at a white vertex $\mathbf{w} = m\hat{x} + n\hat{y}$ and $F(\mathbf{b}) = a(bz/a)^{-m} (cw/bz)^{-n}$ at a black vertex $\mathbf{b} = e_1 + m\hat{x} + n\hat{y}$. These functions are defined on all of the honeycomb graph \mathcal{H} .

Lemma 3.1 *We have*

$$K_{\mathcal{H}} F = F K_{\mathcal{H}} = 0 \quad (4)$$

where $K_{\mathcal{H}}$ is the adjacency matrix of \mathcal{H} .

Proof: This follows from the equation $a + bz + cw = 0$. □

Note that $K_{\mathcal{H}}$ is also a Kasteleyn matrix for \mathcal{H} .

Define a 1-form Ω on edges of \mathcal{H} by

$$\Omega(\mathbf{wb}) = -\Omega(\mathbf{bw}) = 2\epsilon \operatorname{Re}(F(\mathbf{w}))F(\mathbf{b}). \quad (5)$$

By (4) the dual form Ω^* (defined by $\Omega^*((wb)^*) = \Omega(wb)$) is closed (the integral around any closed cycle is zero) and therefore Ω^* is the gradient of a complex-valued function Ψ on \mathcal{H}^* . Extend Ψ linearly over the edges of \mathcal{H}^* . This defines a mapping from \mathcal{H}^* to \mathbb{C} (and by restriction, of \mathcal{G}^* to \mathbb{C}) with the property that the images of the white faces are **non-overlapping** triangles similar to the a, b, c -triangle (via orientation-preserving similarities), and the images of black faces are segments. See [12], Section 5 for the proof of the non-overlapping property, or look at Figure 9. It may be that $\operatorname{Re}F(\mathbf{w}) = 0$ for some \mathbf{w} ; in this case choose a generic modulus-1 complex number λ and replace $F(\mathbf{w})$ by $\lambda F(\mathbf{w})$ and $F(\mathbf{b})$ by $\bar{\lambda} F(\mathbf{b})$.

The mapping Ψ is approximately linear, in fact it is a linear map $\phi(m, n) = \epsilon(cwm + an)$ plus an oscillating (bounded) mapping. To see this, consider for example a vertical column of horizontal edges $\{\mathbf{w}_1 \mathbf{b}_1, \dots, \mathbf{w}_k \mathbf{b}_k\}$ of \mathcal{H} connecting a face f_1 to face f_{k+1} . We have

$$\begin{aligned} \sum_{i=1}^k \Omega(\mathbf{w}_i \mathbf{b}_i) &= \epsilon \sum_{i=1}^k (F(\mathbf{w}_i) + \overline{F(\mathbf{w}_i)}) F(\mathbf{b}_i) \\ &= \epsilon k a + \epsilon \sum_{i=1}^k \overline{F(\mathbf{w}_i)} F(\mathbf{b}_i) \\ &= \phi(f_{k+1}) - \phi(f_1) + \text{osc}, \end{aligned} \quad (6)$$

where osc is oscillating and in fact $O(\epsilon)$ independently of k . In the other two lattice directions the linear part of Ψ is again ϕ .

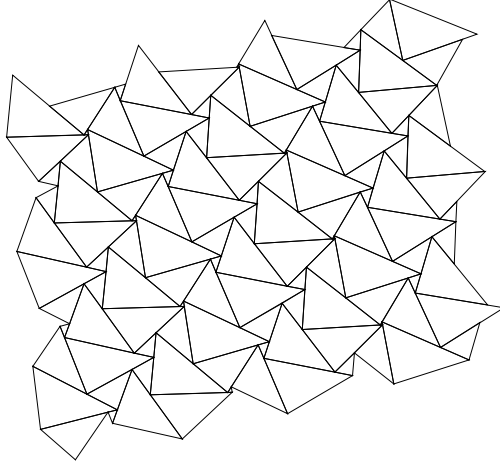


Figure 9: The Ψ -image of \mathcal{H}^* is a T -graph covering \mathbb{R}^2

This shows that the image of \mathcal{H}^* under Ψ is an infinite T -graph \mathcal{H}_T covering all of \mathbb{R}^2 . The images of the black triangles are the complete edges and have lengths $O(\epsilon)$. The image of \mathcal{G}^* under Ψ is a finite sub- T -graph \mathcal{G}_T .

If we insert a λ as above and let λ vary over the unit circle, one sees all possible local structures of the T -graph, that is, the geometry of the T -graph in a neighborhood of $\Psi(\mathbf{w})$ only depends up to homothety on the argument of $\lambda F(\mathbf{w})$.

The union of the Ψ -images of the white triangles in \mathcal{G}^* forms a polygon P . Define the graphs \mathcal{H}_D associated to \mathcal{H}_T , and \mathcal{G}_D associated to \mathcal{G}_T as in section 2.5.2. See Figure 7 for the T -graph arising from the graph \mathcal{G}^* of Figure 5. Note that \mathcal{G}_D contains \mathcal{G} but has extra white vertices along the boundaries.

From (5) we have

Lemma 3.2 *Edge weights of \mathcal{H}_D and \mathcal{G}_D are gauge equivalent to constant edge weights. Indeed, we have $K_{\mathcal{G}_D}(\mathbf{w}, \mathbf{b}) = 2\epsilon \operatorname{Re}(F(\mathbf{w}))F(\mathbf{b})K_{\mathcal{G}}(\mathbf{w}, \mathbf{b})$ and similarly for $K_{\mathcal{H}_D}$.*

Asymptotics of $K_{\mathcal{G}_D}^{-1}$ are described below in section 3.4. For $K_{\mathcal{H}_D}$, from (2) we have

$$K_{\mathcal{H}_D}^{-1}(\mathbf{b}, \mathbf{w}) = \frac{1}{2\pi \operatorname{Re}(F(\mathbf{w}))F(\mathbf{b})} \operatorname{Im} \left(\frac{F(\mathbf{w})F(\mathbf{b})}{\phi(\mathbf{b}) - \phi(\mathbf{w})} \right) + O\left(\frac{\epsilon}{|\phi(\mathbf{b}) - \phi(\mathbf{w})|^2}\right) \quad (7)$$

because $K_{\mathcal{H}_D}$ is gauge-equivalent to K_{ν} . Note that the factor ϵ is absorbed in the mapping ϕ .

3.2 Boundary behavior

In this section we show that the normalized boundary height function of \mathcal{G}_D when \mathcal{G}_D is chosen as above approximates \bar{h} . This is proved in a roundabout way: we first show that the boundary height does not depend (up to local fluctuations) on the exact choice

of boundary conditions (as long as we construct \mathcal{G}_T from \mathcal{G}^* as in section 2.1). Then we compute the height change for “simple” boundary conditions.

3.2.1 Flows and dimer configurations

Any dimer configuration m defines a flow (1-form) $[m]$ with source 1 at each white vertex and sink 1 at each black vertex: flow by 1 along each edge in m and 0 on the other edges.

The set $\Omega_1 \subset [0, 1]^E$ of unit white-to-black flows with capacity 1 on each edge is a convex polytope whose vertices are the dimer configurations [13]. On the graph \mathcal{H} define the flow $\omega_{1/3} \in \Omega_1$ to be the flow with value $1/3$ on each edge wb from w to b . Up to a factor $1/3$, this flow defines the height function, in the sense that for any dimer configuration m , $[m] - \omega_{1/3}$ is a divergence-free flow and the integral of its dual (which is closed) is $1/3$ times the height function of m (see [10]). That is, the height difference between two points is three times the flux of $[m] - \omega_{1/3}$ between those points.

For a finite subgraph of \mathcal{H} the *boundary* height function can be obtained by integrating around the boundary (3 times) the dual of $[m] - \omega_{1/3}$ for some m .

3.2.2 Canonical flow

On \mathcal{H}_D there is a canonical flow $\omega \in \Omega_1$ defined as illustrated in Figure 10: let $v_1 v_2$ be the two vertices of \mathcal{G}_T along b adjacent to w . The flow from w to b is $1/(2\pi)$ times the sum of the two angles that the complete edges through v_1 and v_2 make with b . One or both of these angles may be zero.

Note that the total flow out of w is 1. For an edge b , the total flow into b is also 1 as illustrated on the right in Figure 10.

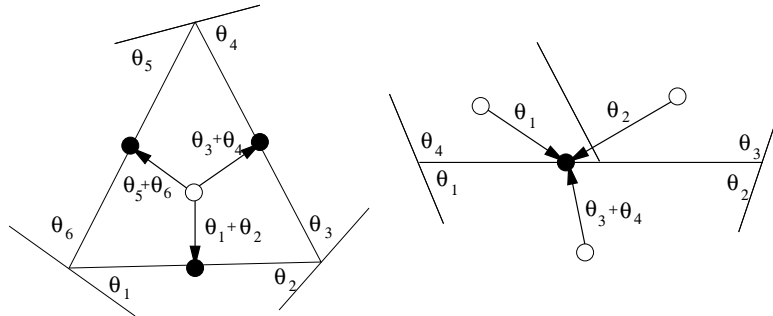


Figure 10: Defining the canonical flow (divide the angles by 2π).

Along the boundary the divergence of $[m] - \omega$ for any dimer configuration m is easily calculated: it is just the turning angle of the boundary. In particular it is bounded.

3.2.3 Boundary height

Now the flux of $\omega_{1/3} - \omega$ defines the boundary height function up to $O(1)$ (the turning of the boundary), since the flux of $[m] - \omega$ is the boundary turning angle. The flux of $\omega_{1/3} - \omega$ can be computed along a path near the boundary, and in fact because both $\omega_{1/3}$ and ω are locally defined from \mathcal{H}_D , we see that the flux does not depend on the exact choice of the nearby boundary. In particular we can calculate the flux, that is, the boundary height change, for a particularly nice choice of boundary and that will tell us the height change between the same points for general boundary conditions.

So let us suppose that part of the boundary is exactly vertical (in the \hat{y} direction) in \mathcal{G}^* . Take a vertical column of horizontal edges in \mathcal{G} . The Ψ image of the dual of this column is a polygonal curve whose j th edge is (using (6)) a constant times $1 + (\frac{z}{w})^{2j}$. It has a non-convex corner when both

$$\operatorname{Im}\left(\left(\frac{z}{w}\right)^{2j}\right) > 0 \quad \text{and} \quad \operatorname{Im}\left(\left(\frac{z}{w}\right)^{2j+2}\right) < 0.$$

The image of the triangles in a vertical column of \mathcal{G}^* is as shown in Figure 11.

The boundary of the graph \mathcal{G}_D then resembles the upper or lower boundary in Figure 12 (which is rotated by 90° to fit on the page). That is, it consists of \mathcal{G} with

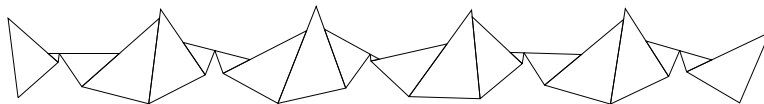


Figure 11: A column of triangles from \mathcal{G}_T .

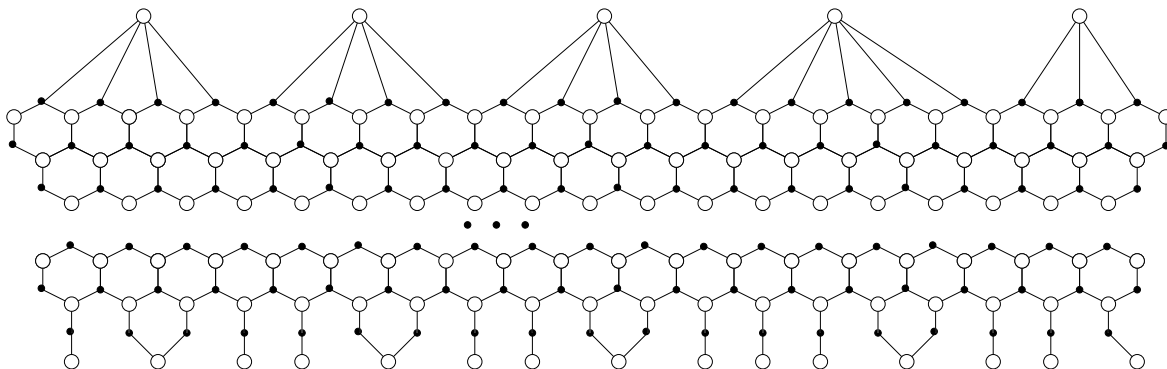


Figure 12: Extra vertices along the boundary of \mathcal{G} . The upper figure gives the vertices which would arise if the upper boundary of Figure 11 were the boundary of \mathcal{G}_T . The lower represents those which would come from the lower boundary of Figure 11.

extra white vertices glued along the boundary in a quasiperiodic fashion. There is a

white vertex glued to a sequence of black vertices corresponding to a maximal sequence of nonconvex corners of \mathcal{G}_T .

The height function decreases by 1 along each segment of \mathcal{G}^* except at a nonconvex corner (of \mathcal{G}_T) where it increases by 2 instead. In particular the slope of the height function in the vertical direction is $3p - 1$ where p is the probability that the argument of $(z/w)^{2j}$ is in the interval $[\pi - \theta, \pi)$, that is, $p = \frac{2}{\pi} \arg z/w = 2\theta_a/2\pi = p_a$. A similar argument holds in the other two directions, and shows that the normalized height function has normal (p_a, p_b, p_c) .

3.3 Continuous and discrete harmonic functions

To understand the asymptotic expansions of G^* , we need to understand asymptotic expansions (as $\epsilon \rightarrow 0$) of general harmonic functions on \mathcal{H}_T .

3.3.1 Smooth functions

Constant and linear functions on \mathbb{R}^2 , when restricted to \mathcal{H}_T , are exactly harmonic. More generally, if we take a (continuous) harmonic function f on \mathbb{R}^2 and evaluate it on the vertices of \mathcal{H}_T , the result will be close to a discrete harmonic function f_ϵ , in the sense that the discrete Laplacian will be $O(\epsilon^2)$:

$$f(v) - \frac{d_2}{d_1 + d_2} f(v - \epsilon d_1 e^{i\theta}) - \frac{d_1}{d_1 + d_2} f(v + \epsilon d_2 e^{i\theta}) = O(\epsilon^2).$$

This situation is not as good as in the (more standard) case of a graph like $\epsilon\mathbb{Z}^2$, where if we evaluate a continuous harmonic function on the vertices, the Laplacian of the resulting discrete function is $O(\epsilon^4)$.

In the present case the principal error is due to the second derivatives of f . To get an error smaller than $O(\epsilon^2)$ for the discrete harmonic function, we need to add an extra term. If we add to f a term which is ϵ^2 times a (bounded but oscillating) function on the vertices of \mathcal{H}_T , it is possible to improve the error in the Laplacian to $O(\epsilon^3)$ (and similarly, higher derivatives of f will contribute lower-order corrections). In fact we can add ϵ^2 times a bounded function f_2 whose value at a point v depends only on the local structure of \mathcal{H}_T near v and on the 2-jet of f . The idea is simple: we just need to add to f (restricted to \mathcal{H}_T) a bounded function on \mathcal{H}_T whose \mathcal{H}_T -Laplacian equals the negative of the \mathcal{H}_T -Laplacian of f , up to $O(\epsilon^3)$. That is, to find a discrete harmonic function f_ϵ asymptotic to f as $\epsilon \rightarrow 0$, we have for $x \in \mathcal{H}_T$

$$f_\epsilon(x) = f(x) + \epsilon^2 f_2(x) + O(\epsilon^3),$$

where $f_2(x)$ depends on the 2-jet of f at x and on the local structure of the graph \mathcal{H}_T at x .

The existence of such a function f_2 follows from the asymptotic formula (7) for K^{-1} , or more precisely from its integral which gives the discrete conjugate Green's function $G^*(w, v)$. That is, we can compare the discrete and continuous versions of the conjugate Green's function, and derive from them the dependence of *any* discrete

harmonic function on its smooth counterpart. The idea is that as v varies the 2-jet of $\text{Im} \log(v - \mathbf{w})$ (modulo the constant and linear terms) takes all possible values for the 2-jet of a harmonic function. Moreover as λ varies over the unit circle it takes all possible values at all possible local structures of \mathcal{H}_T .

The actual formula for f_2 will not interest us here (see however [8], Theorem 4.3) since we only need the existence of the approximation to the discrete harmonic function.

Lemma 3.3 *For a smooth harmonic function f on \mathbb{R}^2 there is a discrete harmonic function f_ϵ on \mathcal{H}_T such that*

$$f_\epsilon(x) = f(x) + O(\epsilon^2),$$

where the constant in the $O(\epsilon^2)$ term depends on the second derivatives of f at x .

3.3.2 Discrete and continuous Green's functions

There is another difference between the discrete and continuous conjugate Green's functions, due to that fact that the continuous Green's function $g^*(w, v)$ is not smooth near $w = v$.

The continuous conjugate Green's function on the whole plane is

$$g^*(w, v) = \frac{1}{2\pi} \text{Im} \log(v - w).$$

To compute the discrete conjugate Green's function G^* , if we simply restrict the continuous Green's function to the vertices of \mathcal{H}_T , it will be very nearly harmonic as a function of v for large $|v - w|$, but the discrete Laplacian of g^* at vertices v near w (within $O(\epsilon)$ of w) will be of constant order in general. So we can expect the long-range behavior of the discrete conjugate Green's function $G^*(\mathbf{w}, v)$ to be equal to g^* plus a sum of terms involving the real part $\text{Re} \log(v - v_j)$ for v_j within $O(\epsilon)$ of w . These extra terms sum to a function of the form $c \log |v - \mathbf{w}| + \epsilon s(v) + O(\epsilon^2)$, where s is a smooth function and c is a constant, both c and s depending on the local structure of \mathcal{H}_T near w .

This form of G^* can be seen explicitly, of course, if we integrate the exact formula (7). We have

Lemma 3.4 *The discrete conjugate Green's function G^* on the plane \mathcal{H}_T is asymptotically*

$$\begin{aligned} G^*(\mathbf{w}, v) &= \frac{1}{2\pi} \left(\text{Im} \log(\phi(v) - \phi(\mathbf{w})) + \frac{\text{Im}(F(\mathbf{w}))}{\text{Re}(F(\mathbf{w}))} \text{Re} \log(\phi(v) - \phi(\mathbf{w})) \right) + \epsilon s(\mathbf{w}, v) + O(\epsilon^2) \\ &= \frac{1}{2\pi \text{Re}(F(\mathbf{w}))} \text{Im}(F(\mathbf{w}) \log(\phi(v) - \phi(\mathbf{w}))) + \epsilon s(\mathbf{w}, v) + O(\epsilon^2) \end{aligned}$$

where $s(\mathbf{w}, v)$ is a smooth function of v .

Proof: From the argument of the previous paragraph, it suffices to compute the constant in front of the $\text{Re} \log(\phi(v) - \phi(w))$ term. This can be computed by differentiating the above formula and comparing with formula (7) for K^{-1} .

The differential of $\epsilon s(w, v)$ is $O(\epsilon)$. Let v_1, v_2 be two vertices of complete edge \mathbf{b} , coming from adjacent faces of \mathcal{H} , adjacent across an edge \mathbf{bw}_1 (so that $v_1 - v_2 = \Omega^*(\mathbf{bw}_1) = 2\epsilon \text{Re}(F(w_1))F(\mathbf{b})$). We have for w far from w_1

$$\begin{aligned} K_{\mathcal{H}_D}^{-1}(\mathbf{b}, w) &= \frac{G^*(w, v_1) - G^*(w, v_2)}{v_1 - v_2} \\ &= \frac{\frac{1}{2\pi} \text{Im} \left(\frac{F(w)}{\text{Re}(F(w))} \frac{v_1 - v_2}{\phi(\mathbf{b}) - \phi(w)} \right)}{2\epsilon \text{Re}(F(w_1))F(\mathbf{b})} + O(\epsilon) \\ &= \frac{1}{2\pi \text{Re}(F(w))F(\mathbf{b})} \text{Im} \left(\frac{F(w)F(\mathbf{b})}{\phi(\mathbf{b}) - \phi(w)} \right) + O(\epsilon). \end{aligned}$$

□

3.4 $K_{\mathcal{G}_D}^{-1}$ in constant-slope case

Theorem 3.5 *In the case of constant slope ν and a bounded domain U , let ξ be a conformal diffeomorphism from $\phi(U)$ to \mathbb{H} . When \mathbf{b} and w are converging to different points as $\epsilon \rightarrow 0$ we have*

$$K_{\mathcal{G}_D}^{-1}(\mathbf{b}, w) = \frac{1}{2\pi \text{Re}(F(w))F(\mathbf{b})} \text{Im} \left(\frac{\xi'(\phi(\mathbf{b}))F(w)F(\mathbf{b})}{\xi(\phi(\mathbf{b})) - \xi(\phi(w))} + \frac{\xi'(\phi(\mathbf{b}))\overline{F(w)}F(\mathbf{b})}{\xi(\phi(\mathbf{b})) - \overline{\xi(\phi(w))}} \right) + O(\epsilon). \quad (8)$$

Proof: The continuous conjugate Green's function on $\phi(U)$ is

$$g^*(z_1, z_2) = \frac{1}{2\pi} \text{Im} \log(\xi(z_1) - \xi(z_2)) + \frac{1}{2\pi} \text{Im} \log(\xi(z_1) - \overline{\xi(z_2)}).$$

From this we construct $K_{\mathcal{G}_D}^{-1}$. The discretization of the first term in g^* is the same as the discretization of the continuous conjugate Green's function on the whole plane (see the calculation in the proof of Lemma 3.4, except replacing ϕ with $\xi \circ \phi$). This gives the first term in (8).

The second term in (8) arises from the continuous harmonic function of v whose boundary values are minus the boundary values of the first term—since we want $G^*(w, v) = 0$ when $\xi(\phi(v))$ is real. So we have

$$G^*(w, v) = \frac{1}{2\pi} \left(\frac{F(w)}{\text{Re}(F(w))} \text{Im} \log(\xi(\phi(v)) - \xi(\phi(w))) - \frac{\overline{F(w)}}{\text{Re}(F(w))} \text{Im} \log(\xi(\phi(v)) - \overline{\xi(\phi(w))}) \right) + \epsilon S(w, v) + O(\epsilon^2) \quad (9)$$

where S is smooth. Differentiating gives the result. □

Note that when \mathbf{b} is within $O(\epsilon)$ of \mathbf{w} , and neither is close to the boundary, the discrete Green's function $G^*(\mathbf{w}, v)$ for v on \mathbf{b} is equal to the discrete Green's function on the plane $G_{\mathcal{H}_T}^*(\mathbf{w}, v)$ plus an error which is $O(1)$ coming from the corrective term due to the boundary. The error is smooth plus oscillations of order $O(\epsilon^2)$, so that within $O(\epsilon)$ of \mathbf{w} the error is a linear function plus $O(\epsilon)$. Therefore when we take derivatives

$$K_{\mathcal{G}_D}^{-1}(\mathbf{b}, \mathbf{w}) = K_{\mathcal{H}_D}^{-1}(\mathbf{b}, \mathbf{w}) + O(1),$$

which, since $K_{\mathcal{H}_D}^{-1}$ is of order $O(\epsilon^{-1})$ when $|\mathbf{b} - \mathbf{w}| = O(\epsilon)$, implies that the local statistics are given by μ_ν .

Theorem 3.6 *In the case of constant slope, the local statistics at any point in the interior of U are given in the limit $\epsilon \rightarrow 0$ by μ_ν , the ergodic Gibbs measure on tilings of the plane of slope ν .*

4 General boundary conditions

Here we consider the general setting: U is a smooth Jordan domain and \bar{h} , the normalized asymptotic height function on U , is not necessarily linear.

4.1 The complex height function

Lemma 4.1 ([9]) *Let a, b, c, z, w be defined from \bar{h} as in section 2.2, where \bar{h} is the normalized asymptotic height function on U . Then $\Phi = -cw/a$ satisfies the complex Burger's equation*

$$\Phi_x = -\Phi\Phi_y. \tag{10}$$

The equation (10) implies that the form

$$\log(\Phi - 1)dx - \log\left(\frac{1}{\Phi} - 1\right)dy$$

is closed. Since U is simply connected it is in fact exact: there is a function $H: U \rightarrow \mathbb{C}$ satisfying

$$dH = \log(\Phi - 1)dx - \log\left(\frac{1}{\Phi} - 1\right)dy.$$

We call H the **complex height function**. Its imaginary part is related to \bar{h} : from (1) we have

$$-\text{Im}H = \frac{\pi}{3}\left(\frac{\bar{h}}{\sqrt{2}} - 2x - y\right) + \text{const.}$$

The real part of H is the logarithm of a special gauge function which we describe below.

We have

$$H_x = \log(\Phi - 1) \quad (11)$$

$$H_y = -\log\left(\frac{1}{\Phi} - 1\right) \quad (12)$$

$$H_{xx} = \frac{\Phi_x}{\Phi - 1} = \frac{-\Phi\Phi_y}{\Phi - 1} \quad (13)$$

$$H_{yy} = -\frac{1}{\Phi - 1} \frac{\Phi_y}{\Phi}. \quad (14)$$

4.2 Gauge transformation

The mapping Φ is a real analytic mapping from U to the upper half plane. It is an open mapping since $\text{Im}(\Phi_x/\Phi_y) = -\text{Im}\Phi \neq 0$, but may have isolated critical points. Let ϕ be a diffeomorphism from U onto the upper half plane satisfying the Beltrami equation

$$\frac{\frac{d\phi}{d\bar{z}}}{\frac{d\phi}{dz}} = \frac{\frac{d\Phi}{d\bar{z}}}{\frac{d\Phi}{dz}} = \frac{-\Phi + i}{-\Phi - i},$$

that is $\phi_x = -\Phi\phi_y$. Such a ϕ exists by the Ahlfors-Bers theorem [1]. It follows that Φ is of the form $f(\phi)$ for some holomorphic function f from \mathbb{H} into \mathbb{H} . Since ∂U is smooth, ϕ is smooth up to and including the boundary.

For white vertices of \mathcal{G} define

$$F(\mathbf{w}) = e^{\frac{1}{\epsilon}H(\mathbf{w})} \sqrt{\phi_y(\mathbf{w})} (1 + \epsilon M(\mathbf{w})),$$

where $M(\mathbf{w})$ is any function which satisfies

$$e^{-H_x} M_x - e^{H_y} M_y = e^{-H_x} \left(\frac{H_{xx}^2}{8} - \frac{H_{xxx}}{6} - \frac{H_{xx}\phi_{xy}}{4\phi_y} - \frac{\phi_{xy}^2}{8\phi_y^2} + \frac{\phi_{xyy}}{4\phi_y} \right) + e^{H_y} \left(\frac{H_{yy}^2}{8} + \frac{H_{yyy}}{6} + \frac{H_{yy}\phi_{yy}}{4\phi_y} - \frac{\phi_{yy}^2}{8\phi_y^2} + \frac{\phi_{yyy}}{4\phi_y} \right). \quad (15)$$

The existence of such an M follows from the fact that the ratio of the coefficients of M_x and M_y is $-e^{H_x+H_y} = \Phi$, so (15) is of the form

$$M_x + \Phi M_y = J(x, y)$$

for some smooth function J . This is the $\bar{\partial}$ equation in coordinate ϕ .

For black vertices \mathbf{b} define

$$F(\mathbf{b}) = e^{-\frac{1}{\epsilon}H(\mathbf{w})} \sqrt{\phi_y(\mathbf{w})} (1 - \epsilon M(\mathbf{w})),$$

where \mathbf{w} is the vertex adjacent to and left of \mathbf{b} and $M(\mathbf{w})$ is as above.

Lemma 4.2 For each black vertex \mathbf{b} with three neighbors in \mathcal{G} we have

$$\sum_{\mathbf{w}} F(\mathbf{w})K(\mathbf{w}, \mathbf{b}) = O(\epsilon^3)$$

and for each white vertex \mathbf{w} we have

$$\sum_{\mathbf{b}} K(\mathbf{w}, \mathbf{b})F(\mathbf{b}) = O(\epsilon^3).$$

Proof: This is a calculation. Let $\mathbf{w}, \mathbf{w} - \epsilon\hat{x}, \mathbf{w} + \epsilon\hat{y}$ be the three neighbors of \mathbf{b} . Then, setting $H = H(\mathbf{w})$, $\phi_y = \phi_y(\mathbf{w})$, and $M = M(\mathbf{w})$ we have

$$F(\mathbf{w} - \epsilon\hat{x}) = e^{\frac{1}{\epsilon}(H - \epsilon H_x + \frac{\epsilon^2}{2}H_{xx} - \frac{\epsilon^3}{6}H_{xxx} + O(\epsilon^4))} \sqrt{\phi_y - \epsilon\phi_{yx} + \frac{\epsilon^2}{2}\phi_{yxx} + O(\epsilon^3)}(1 + \epsilon M - \epsilon^2 M_x + O(\epsilon^3))$$

$$F(\mathbf{w} + \epsilon\hat{y}) = e^{\frac{1}{\epsilon}(H + \epsilon H_y + \frac{\epsilon^2}{2}H_{yy} + \frac{\epsilon^3}{6}H_{yyy} + O(\epsilon^4))} \sqrt{\phi_y + \epsilon\phi_{yy} + \frac{\epsilon^2}{2}\phi_{yyy} + O(\epsilon^3)}(1 + \epsilon M + \epsilon^2 M_y + O(\epsilon^3)).$$

The sum of the leading order terms in $F(\mathbf{w}) + F(\mathbf{w} - \epsilon\hat{x}) + F(\mathbf{w} + \epsilon\hat{y})$ is

$$e^{\frac{1}{\epsilon}H} \sqrt{\phi_y}(1 + e^{-H_x} + e^{H_y}) = e^{\frac{1}{\epsilon}H} \sqrt{\phi}(1 + \frac{1}{\Phi - 1} + \frac{\Phi}{1 - \Phi}) = 0.$$

The sum of the terms of order ϵ is $\frac{\epsilon}{2}e^{\frac{1}{\epsilon}H} \sqrt{\phi_y}$ times

$$\begin{aligned} & e^{-H_x} \left(-\frac{\phi_{yx}}{\phi_y} + H_{xx} \right) + e^{H_y} \left(\frac{\phi_{yy}}{\phi_y} + H_{yy} \right) = \\ & = \frac{1}{\Phi - 1} \left(\frac{\Phi\phi_{yy}}{\phi_y} + \Phi_y + \frac{-\Phi\Phi_y}{\Phi - 1} \right) + \frac{\Phi}{1 - \Phi} \left(\frac{\phi_{yy}}{\phi_y} - \frac{\Phi_y}{\Phi(\Phi - 1)} \right) = 0 \end{aligned}$$

and the sum of the order- ϵ^2 terms is $\epsilon^2 e^{\frac{1}{\epsilon}H} \sqrt{\phi_y}$ times

$$\begin{aligned} & -e^{-H_x} M_x + e^{H_y} M_y + e^{-H_x} \left(\frac{H_{xx}^2}{8} - \frac{H_{xxx}}{6} - \frac{H_{xx}\phi_{xy}}{4\phi_y} - \frac{\phi_{xy}^2}{8\phi_y^2} + \frac{\phi_{xyy}}{4\phi_y} \right) + \\ & e^{H_y} \left(\frac{H_{yy}^2}{8} + \frac{H_{yyy}}{6} + \frac{H_{yy}\phi_{yy}}{4\phi_y} - \frac{\phi_{yy}^2}{8\phi_y^2} + \frac{\phi_{yyy}}{4\phi_y} \right) = 0. \quad (16) \end{aligned}$$

A similar calculation holds at a white vertex, and we get the same expression for the ϵ^2 contribution (changing the signs of $M, H, d/dx$ and d/dy gives the same expression). \square

It is clear from the proof that the error in the statement can be improved to any order $O(\epsilon^{3+k})$ by replacing $M(\mathbf{w})$ with $M_0(\mathbf{w}) + \epsilon M_1(\mathbf{w}) + \dots + \epsilon^k M_k(\mathbf{w})$, where each M_j satisfies an equation of the form (15) except with a different right hand side—the right-hand side will depend on derivatives of H, ϕ and the M_i for $i < j$. For our proof below we need an error $O(\epsilon^4)$ and therefore the M_0 and M_1 terms, even though the final result will depend on neither M_0 nor M_1 .

4.3 Embedding

Define a 1-form

$$\Omega(\mathbf{wb}) = 2\operatorname{Re}(F(\mathbf{w}))F(\mathbf{b})K(\mathbf{w}, \mathbf{b})$$

on edges of \mathcal{G} (since $K(\mathbf{w}, \mathbf{b}) = \epsilon$ is a constant, this is an unimportant factor for now, but in a moment we will perturb K). By the comments after the proof of Lemma 4.2, the dual form Ω^* on \mathcal{G}^* can be chosen to be closed up to $O(\epsilon^4)$ and so there is a function $\tilde{\phi}$ on \mathcal{G}^* , defined up to an additive constant, satisfying $d\tilde{\phi} = \Omega^* + O(\epsilon^3)$.

In fact up to the choice of the additive constant, $\tilde{\phi}$ is equal to ϕ plus an oscillating function. This can be seen as follows. For a horizontal edge \mathbf{wb} we have $F(\mathbf{w})F(\mathbf{b}) = \phi_y(\mathbf{w}) + O(\epsilon)$. Thus on a vertical column $\{\mathbf{w}_1\mathbf{b}_1, \dots, \mathbf{w}_k\mathbf{b}_k\}$ of horizontal edges we have

$$\sum_{i=1}^k \Omega^*(\mathbf{w}_i\mathbf{b}_i) = \epsilon \sum_{i=1}^k (F(\mathbf{w}_i) + \overline{F(\mathbf{w}_i)})F(\mathbf{b}_i) = \epsilon \sum \phi_y(\mathbf{w}_i) + \epsilon \sum_{i=1}^k \overline{F(\mathbf{w}_i)}F(\mathbf{b}_i) + O(\epsilon^2).$$

The first sum gives the change in ϕ from one endpoint of the column to the other, and the second sum is oscillating ($\overline{F(\mathbf{w}_i)}$ and $F(\mathbf{b}_i)$ have the same argument which is in $(0, \pi)$ and which is a continuous function of the position) and so contributes $O(\epsilon)$. Similarly, in the other two lattice directions the sum is given by the change in ϕ plus an oscillating term.

Therefore by choosing the additive constant appropriately, $\tilde{\phi}$ maps \mathcal{G}^* to a small neighborhood of \mathbb{H} (in the spherical metric), which shrinks to \mathbb{H} as $\epsilon \rightarrow 0$.

The map $\tilde{\phi}$ has the following additional properties. The image of the three edges of a black face of \mathcal{G}^* are nearly collinear, and the image of a white triangle is a triangle nearly similar to the a, b, c -triangle, and of the same orientation. Thus it is nearly a mapping onto a T -graph. In fact near a point where the relative weights are a, b, c -weights which are slowly varying on the scale of the lattice—the map is up to errors the map of section 3.

We can adjust the mapping $\tilde{\phi}$ by $O(\epsilon^3)$ so that the image of each black triangle is an exact line segment: this can be arranged by choosing for each black face a line such that the $\tilde{\phi}$ -image of the corresponding black face is within $O(\epsilon^3)$ of that line; the intersections of these lines can then be used to define a new mapping $\Psi: \mathcal{G}^* \rightarrow \mathbb{C}$ which is an exact T -graph mapping.

The mapping Ψ will then correspond to the above 1-form Ω but for a matrix \tilde{K} with slightly different edge weights. Let us check how much the weights differ from the original weights (which are ϵ). As long as the triangular faces are of size of order ϵ (which they are typically), the adjustment will change the edge lengths locally by $O(\epsilon^3)$ and therefore their relative lengths by $1 + O(\epsilon^2)$. There will be some isolated triangular faces, however, which will be smaller—of order $O(\epsilon^2)$ because of the possibility that $F(\mathbf{w})$ might be nearly pure imaginary. We can deal with these as follows. Once we have readjusted the “large” triangular faces we have an exact T -graph mapping on most of the graph. We can then multiply $F(\mathbf{w})$ by $\lambda = i$ and $F(\mathbf{b})$ by $\bar{\lambda} = -i$: the readjusted weights give (for most of the graph) a new exact T -graph mapping (because we now have $\tilde{K}F = F\tilde{K} = 0$ exactly for these weights), but now all faces which were too small

before become $O(\epsilon)$ in size and we can readjust their dimensions locally by a factor $1 + O(\epsilon^2)$.

In the end we have an exact mapping Ψ of \mathcal{G}^* onto a T -graph \mathcal{G}_T and it distorts the edge weights of K by at most $1 + O(\epsilon^2)$. We shall see in section 5 that this is close enough to get a good approximation to K^{-1} .

The Kasteleyn matrix for \mathcal{G}_D is equal to $\tilde{K}(\mathbf{w}, \mathbf{b})F(\mathbf{b})2\text{Re}(F(\mathbf{w}))$ where \tilde{K} has edge weights $\epsilon + O(\epsilon^3)$.

4.4 Boundary

Along the boundary we claim that the normalized height function of \mathcal{G}_D follows u . Since \mathcal{G}_D arises from a T -graph, we can use its canonical flow (section 3.2.2). Near any given point the canonical flow looks like the canonical flow in the constant-weight case—since the weights vary continuously, they vary slowly at the scale ϵ , the scale of the graph. Since the canonical flow defines the slope of the normalized height function, we have pointwise convergence of the derivative of \bar{h} along the boundary to the derivative of u . Thus \bar{h} converges to u . In fact this argument shows that the normalized height function of the canonical flow converges to the asymptotic height function in the interior of U as well.

5 Continuity of K^{-1}

In this section we show how K^{-1} changes under a small change in edge weights.

Lemma 5.1 *Suppose $0 < \delta \ll \epsilon$. If \mathcal{G}' is a graph identical to \mathcal{G}_D but with edge weights which differ by a factor $1 + O(\delta)$, then*

$$K_{\mathcal{G}_D}^{-1} = K_{\mathcal{G}'}^{-1}(1 + O(\delta/\epsilon)).$$

In particular since $\delta = \epsilon^2$ in our case this will be sufficient to approximate K^{-1} to within $1 + O(\epsilon)$.

Proof: For any matrix A we have

$$(K + \delta\epsilon A)^{-1} = K^{-1} \left(1 + \sum_{j=1}^{\infty} (-1)^j (\delta\epsilon)^j (AK^{-1})^j \right),$$

as long as this sum converges.

From Theorem 6.1 below we have that $K_{\mathcal{G}'}^{-1}(\mathbf{b}, \mathbf{w}) = O(1/|\mathbf{b} - \mathbf{w}|)$. When A represents a bounded, weighted adjacency matrix of \mathcal{G}_D , the matrix norm of AK^{-1} is then

$$\|AK^{-1}\| \leq \max_{\mathbf{w}'} \sum_{\mathbf{w}} \left| \sum_{\mathbf{b}} A(\mathbf{w}', \mathbf{b})K^{-1}(\mathbf{b}, \mathbf{w}) \right| \leq 3a \max_{\mathbf{w}'} \sum_{\mathbf{w} \neq \mathbf{w}'} \frac{1}{|\mathbf{w}' - \mathbf{w}|} = O(\epsilon^{-2})$$

where a is the maximum entry of A . In particular when $\delta \ll \epsilon$ we have

$$(K + \delta\epsilon A)^{-1} = K^{-1}(1 + O(\delta/\epsilon)).$$

□

6 Asymptotic coupling function

Theorem 6.1 *If \mathbf{b}, \mathbf{w} are not within $o(1)$ of the boundary of U , we have*

$$K_{\mathcal{G}_D}^{-1}(\mathbf{b}, \mathbf{w}) = \frac{1}{2\pi \operatorname{Re}(F(\mathbf{w}))F(\mathbf{b})} \operatorname{Im} \left(\frac{F(\mathbf{w})F(\mathbf{b})}{\phi(\mathbf{b}) - \phi(\mathbf{w})} + \frac{\overline{F(\mathbf{w})}F(\mathbf{b})}{\phi(\mathbf{b}) - \overline{\phi(\mathbf{w})}} \right) + O(\epsilon). \quad (17)$$

When one or both of \mathbf{b}, \mathbf{w} are near the boundary, but they are not within $o(1)$ of each other, then $K_{\mathcal{G}_D}^{-1}(\mathbf{b}, \mathbf{w}) = O(1)$.

Proof: The proof is identical to the proof in the constant-slope case, see Theorem 3.5, except that $\xi\phi$ there is ϕ here. The ξ' factors from (8) are here absorbed in the definition of the functions ϕ and F . □

As in the case of constant slope, when \mathbf{b} and \mathbf{w} are close to each other (within $O(\epsilon)$) and not within $o(1)$ of the boundary, Theorem 3.6 applies to show that the local statistics are given by μ_ν .

7 Free field moments

As before let ϕ be a diffeomorphism from U to \mathbb{H} satisfying $\phi_x = -\Phi\phi_y$ where Φ is defined from \bar{h} as in section 4.1.

Theorem 7.1 *Let \bar{h} be the asymptotic height function on \mathcal{G}_D , h_ϵ the normalized height function of a random tiling, and $\hat{h} = \frac{2\sqrt{\pi}}{3\epsilon}(h_\epsilon - \bar{h})$. Then \hat{h} converges weakly as $\epsilon \rightarrow 0$ to $\phi^*\mathcal{F}$, the pull-back under ϕ of \mathcal{F} , the Gaussian free field on \mathbb{H} .*

Here weak convergence means that for any smooth test function ψ on U , zero on the boundary, we have

$$\epsilon^2 \sum_{\mathcal{G}_D} \psi(f) \hat{h}(f) \rightarrow \int_U \psi(x) \mathcal{F}(\phi(x)) |dx|^2,$$

where the sum on the left is over faces f of \mathcal{G}_D .

Proof: We compute the moments of \mathcal{F} . Let ψ_1, \dots, ψ_k be smooth functions on U , each zero on the boundary. We have

$$\mathbb{E} \left[\left(\epsilon^2 \sum_{f_1 \in \mathcal{G}_D} \psi_1(f_1) \hat{h}(f_1) \right) \cdots \left(\epsilon^2 \sum_{f_k \in \mathcal{G}_D} \psi_k(f_k) \hat{h}(f_k) \right) \right] =$$

$$= \epsilon^{2k} \sum_{f_1, \dots, f_k} \psi_1(f_1) \cdots \psi_k(f_k) \mathbb{E}[\hat{h}(f_1) \dots \hat{h}(f_k)].$$

From Theorem 7.2 below the sum becomes

$$= \int_U \cdots \int_U \mathbb{E}[\mathcal{F}(\phi(x_1)) \dots \mathcal{F}(\phi(x_k))] \prod \psi_i(x_i) |dx_i|^2 + o(1),$$

that is, the moments of \hat{h} converge to the moments of the free field $\phi^*(\mathcal{F})$. Since the free field is a Gaussian process, it is determined by its moments. This completes the proof. \square

Theorem 7.2 *Let $s_1, \dots, s_k \in U$ be distinct points in the interior of U . For each ϵ let f_1, f_2, \dots, f_k be faces of \mathcal{G}_D , with f_i converging to s_i as $\epsilon \rightarrow 0$. If k is odd we have*

$$\lim_{\epsilon \rightarrow 0} \mathbb{E}[\hat{h}(f_1) \dots \hat{h}(f_k)] = 0$$

and if k is even we have

$$\lim_{\epsilon \rightarrow 0} \mathbb{E}[\hat{h}(f_1) \dots \hat{h}(f_k)] = \sum_{\text{pairings } \sigma} \prod_{j=1}^{k/2} G(\phi(s_{\sigma(2j-1)}), \phi(s_{\sigma(2j)}))$$

where

$$G(z, z') = -\frac{1}{2\pi} \log \left| \frac{z - z'}{z - \bar{z}'} \right|$$

is the Dirichlet Green's function on \mathbb{H} and the sum is over all pairings of the indices.

If two or more of the s_i are equal, we have

$$\mathbb{E}[\hat{h}(f_1) \dots \hat{h}(f_k)] = O(\epsilon^{-\ell}),$$

where ℓ is the number of coincidences (i.e. $k - \ell$ is the number of distinct s_i).

Proof: We first deal with the case that the s_i are distinct. Let $\gamma_1, \dots, \gamma_k$ be pairwise disjoint paths of faces from points s'_i on the boundary to the f_i . We assume that these paths are far apart from each other (that is, as $\epsilon \rightarrow 0$ they converge to disjoint paths). The height $h_\epsilon(f_i)$ can be measured as a sum along γ_i .

We suppose without loss of generality that each γ_i is a polygonal path consisting of a bounded number of straight segments which are parallel to the lattice directions $\hat{x}, \hat{y}, \hat{z}$. In this case, by additivity of the height change along γ_i and linearity of the moment in each index, we may as well assume that γ_i is in a single lattice direction.

Now the change in \hat{h} along γ_i is given by the sum of $a_{ij} - \mathbb{E}(a_{ij})$ where a_{ij} is the indicator function of the j th edge crossing γ_i (with a sign according to the direction of γ_i). So the moment is

$$\mathbb{E}[\hat{h}(f_1) \dots \hat{h}(f_k)] = \sum_{j_1 \in \gamma_1, \dots, j_k \in \gamma_k} \mathbb{E}[(a_{1j_1} - \mathbb{E}[a_{1j_1}]) \dots (a_{kj_k} - \mathbb{E}[a_{kj_k}])].$$

If w_{ij_i}, b_{ij_i} are the vertices of edge a_{ij_i} , this moment becomes (see [6])

$$\sum_{j_1, \dots, j_k} \left(\prod_{i=1}^k K(w_{ij_i}, b_{ij_i}) \right) \begin{vmatrix} 0 & K^{-1}(b_{2j_2}, w_{1j_1}) & \dots & K^{-1}(b_{kj_k}, w_{1j_1}) \\ K^{-1}(b_{1j_1}, w_{2j_2}) & 0 & & \\ \vdots & & \ddots & \vdots \\ K^{-1}(b_{1j_1}, w_{kj_k}) & \dots & K^{-1}(b_{k-1j_{k-1}}, w_{kj_k}) & 0 \end{vmatrix}.$$

In particular, the effect of subtracting off the mean values of the a_{ij_i} is equivalent to cancelling the diagonal terms $K^{-1}(b_{ij_i}, w_{ij_i})$ in the matrix.

Expand the determinant as a sum over the symmetric group. For a given permutation σ , which must be fixed-point free or else the term is zero, we expand out the corresponding product, and sum along the paths. For example if σ is the k -cycle $\sigma = (12 \dots k)$, the corresponding term is

$$\begin{aligned} & \text{sgn}(\sigma) \sum_{j_1, \dots, j_k} \left(\prod_{i=1}^k K(w_{ij_i}, b_{ij_i}) \right) K^{-1}(b_{1j_1}, w_{2j_2}) K^{-1}(b_{2j_2}, w_{3j_3}) \dots K^{-1}(b_{kj_k}, w_{1j_1}) = \\ & = -\left(\frac{-1}{4\pi i}\right)^k \sum_{j_1, \dots, j_k} \left(\frac{F(b_{1j_1})F(w_{2j_2})}{\phi(b_{1j_1}) - \phi(w_{2j_2})} + \frac{F(b_{1j_1})\overline{F(w_{2j_2})}}{\phi(b_{1j_1}) - \phi(w_{2j_2})} - \frac{\overline{F(b_{1j_1})}F(w_{2j_2})}{\phi(b_{1j_1}) - \phi(w_{2j_2})} - \frac{\overline{F(b_{1j_1})}F(w_{2j_2})}{\phi(b_{1j_1}) - \phi(w_{2j_2})} \right) \dots \\ & \dots \left(\frac{F(b_{kj_k})F(w_{1j_1})}{\phi(b_{1j_1}) - \phi(w_{2j_2})} + \frac{F(b_{kj_k})\overline{F(w_{1j_1})}}{\phi(b_{kj_k}) - \phi(w_{1j_1})} - \frac{\overline{F(b_{kj_k})}F(w_{1j_1})}{\phi(b_{kj_k}) - \phi(w_{1j_1})} - \frac{\overline{F(b_{kj_k})}F(w_{1j_1})}{\phi(b_{kj_k}) - \phi(w_{1j_1})} \right) \quad (18) \end{aligned}$$

plus lower-order terms. Multiplying out this product, all 4^k terms have an oscillating coefficient (as some j_i varies) except for the terms in which the pairs $F(b_{ij_i})$ and $F(w_{ij_i})$ in the numerator are either both conjugated or both unconjugated for each i . That is, any term involving $F(b_{ij_i})\overline{F(w_{ij_i})}$ or its conjugate will oscillate as j_i varies and so contribute negligibly to the sum. There are only 2^k terms which survive.

Let z_i denote the point $z_i = \phi(b_{ij_i}) \approx \phi(w_{ij_i})$.

For a term with $F(b_{ij_i})$ and $F(w_{ij_i})$ both conjugated, the coefficient

$$\overline{F(b_{ij_i})F(w_{ij_i})}$$

is equal to $d\overline{z_i}$, otherwise it is equal to dz_i , where dz_i is the amount that ϕ changes when moving by one step along path γ_i , that is, when j_i increases by 1.

So the above term for the k -cycle σ becomes

$$-\left(\frac{-1}{4\pi i}\right)^k \sum_{\varepsilon_1, \dots, \varepsilon_k = \pm 1} \left(\prod_j \varepsilon_j \right) \int_{\phi(\gamma_1)} \dots \int_{\phi(\gamma_k)} \frac{dz_1^{(\varepsilon_1)} \dots dz_k^{(\varepsilon_k)}}{(z_1^{(\varepsilon_1)} - z_2^{(\varepsilon_2)})(z_2^{(\varepsilon_2)} - z_3^{(\varepsilon_3)}) \dots (z_k^{(\varepsilon_k)} - z_1^{(\varepsilon_1)})}$$

plus an error of lower order, where $z_j^{(1)} = z_j$ and $z_j^{(-1)} = \overline{z_j}$, with similar expressions for other σ .

When we now sum over all permutations σ , only the fixed-point free involutions do not cancel:

Lemma 7.3 ([2]) For $n > 2$ let C_n be the set of n -cycles in S_n . Then

$$\sum_{\sigma \in C_n} \prod_{i=1}^n \frac{1}{z_{\sigma(i)} - z_{\sigma(i+1)}} = 0,$$

where the indices are taken cyclically.

Proof: This is true for n odd by antisymmetry (pair each cycle with its inverse). For n even, the left-hand side is a symmetric rational function whose denominator is the Vandermonde $\prod_{i < j} (z_i - z_j)$ and whose numerator is of lower degree than the denominator. Since the denominator is antisymmetric, the numerator must be as well. But the only antisymmetric polynomial of lower degree than the Vandermonde is 0. \square

By the lemma, in the big determinant all terms cancel except those for which σ is a fixed-point free involution. It remains to evaluate what happens for a single transposition, since a general fixed-point free involution σ will be a disjoint product of these:

$$\begin{aligned} & \frac{1}{(4\pi i)^2} \left[\int_{\phi(s'_1)}^{\phi(s_1)} \int_{\phi(s'_2)}^{\phi(s_2)} \frac{dz_1 dz_2}{(z_1 - z_2)^2} - \int_{\phi(s'_1)}^{\phi(s_1)} \int_{\phi(s'_2)}^{\phi(s_2)} \frac{d\bar{z}_1 d\bar{z}_2}{(\bar{z}_1 - \bar{z}_2)^2} - \int_{\phi(s'_1)}^{\phi(s_1)} \int_{\phi(s'_2)}^{\phi(s_2)} \frac{dz_1 d\bar{z}_2}{(z_1 - \bar{z}_2)^2} + \int_{\phi(s'_1)}^{\phi(s_1)} \int_{\phi(s'_2)}^{\phi(s_2)} \frac{d\bar{z}_1 dz_2}{(\bar{z}_1 - z_2)^2} \right] \\ &= \frac{1}{(4\pi i)^2} \int_{\phi(s_1)}^{\phi(s'_1)} \int_{\phi(s_2)}^{\phi(s'_2)} \frac{dz_1 dz_2}{(z_1 - z_2)^2} \\ &= \frac{1}{2\pi} G(\phi(s_1), \phi(s_2)) \end{aligned}$$

where we used $\phi(s'_i) \in \mathbb{R}$.

Now suppose that some of the s_i coincide. We choose paths γ_i as before but suppose that the γ_i are close only at those endpoints where the s_i coincide. Let $\delta = \sqrt{\epsilon}$. For pairs of edges $a_{ij_i}, a_{i'j'_i}$ on different paths, both within δ of such an endpoint we use the bound $K^{-1}(\mathbf{b}, \mathbf{w}) = O(\frac{1}{\epsilon})$, so that the big determinant, multiplied by the prefactor $\prod_i K(\mathbf{w}_{ij_i}, \mathbf{b}_{ij_i})$, is $O(1)$. In the sum over paths the net contribution for each coincidence is then $O(\delta/\epsilon)^2 = O(\epsilon^{-1})$, since this is the number of terms in which both edges of two different paths are near the endpoint. \square

8 Boxed plane partition example

For the boxed plane partition, whose hexagon has vertices

$$\{(1, 0), (1, 1), (0, 1), (-1, 0), (-1, -1), (0, -1)\}$$

in (\hat{x}, \hat{y}) coordinates, see Figure 2, it is shown in [9] that Φ satisfies $(-\Phi x + y)^2 = 1 - \Phi + \Phi^2$, or

$$\Phi(x, y) = \frac{1 - 2xy + \sqrt{4(x^2 - xy + y^2) - 3}}{2(1 - x^2)}$$

for (x, y) inside the circle $x^2 - xy + y^2 \leq 3/4$. Φ maps the region inside the inscribed circle with degree 2 onto the upper half-plane, with critical point $(0, 0)$ mapping to $e^{\pi i/3}$. If we map the half plane to the unit disk with the mapping $z \mapsto \frac{z - e^{\pi i/3}}{z - e^{-\pi i/3}}$, the composition is

$$\frac{\Phi(x, y) - e^{\pi i/3}}{\Phi(x, y) - e^{-\pi i/3}} = \frac{2r^2 - 3 + \sqrt{9 - 12r^2}}{2(y - \bar{\omega}x)^2} \quad (19)$$

(where $r^2 = x^2 - xy + y^2$) which maps circles concentric about the origin to circles concentric about the origin. To see this, note that $z = i(y - \omega x)$ defines the standard conformal structure, and $|z|^2 = x^2 - xy + y^2 = r^2$, so that the right-hand side of the equation (19) is $f(r)/\bar{z}^2$.

Note also that the Beltrami differential of Φ , which is

$$\mu(x, y) = \frac{\Phi_{\bar{z}}}{\Phi_z} = \frac{\Phi - e^{\pi i/3}}{\Phi - e^{-\pi i/3}},$$

satisfies

$$\mu = \frac{\mu_{\bar{z}}}{\mu_z},$$

that is, it is its own Beltrami differential! This is simply a restatement of the PDE (10) in terms of μ .

The diffeomorphism ϕ from the inscribed circle to the unit disk is also very simple, it is just $\phi = \sqrt{\mu}$, or

$$\phi(re^{i\theta}) = \frac{\sqrt{3} - \sqrt{3 - 4r^2}}{2r} e^{i\theta}.$$

The inverse of ϕ which maps \mathbb{D} to U is even simpler: it is

$$\phi^{-1}(z) = \frac{z\sqrt{3}}{1 + |z|^2}.$$

This map can be viewed as the orthogonal projection of a hemisphere onto the plane through its equator, if we identify \mathbb{D} conformally with the upper hemisphere sending 0 to the north pole.

In conclusion if the domain U is the disk $\{(x, y) \mid x^2 - xy + y^2 \leq r^2\}$, where $r^2 < 3/4$, and the height function on the boundary of U is given by the height function \bar{h} of the BPP on ∂U , then the \bar{h} on U will equal the \bar{h} on BPP restricted to U , and the fluctuations of the height function are the pull-back of the Gaussian free field on the disk of radius $\frac{\sqrt{3} - \sqrt{3 - 4r^2}}{2r}$ under ϕ .

References

- [1] L. Ahlfors, L. Bers, Riemann's mapping theorem for variable metrics *Ann. Math* **72** (1960), 385-404.
- [2] C. Boutillier, in preparation.

- [3] H. Cohn, R. Kenyon, J. Propp, A variational principle for domino tilings, *J. AMS* **14** (2001), 297-346.
- [4] H. Cohn, M. Larsen, J. Propp, The shape of a typical boxed plane partition, *New York J. Math* **4** (1998), 137-165.
- [5] Jean-René Geoffroy, in preparation.
- [6] R. Kenyon, Conformal invariance of domino tiling. *Ann. Probab.* **28** (2000), 759-795.
- [7] R. Kenyon, Dominos and the Gaussian free field. *Ann. Probab.* **29** (2001), 1128-1137.
- [8] R. Kenyon, The Laplacian and Dirac operators on critical planar graphs, *Invent. Math.* **150** (2002), 409-439.
- [9] R. Kenyon, A. Okounkov, Limit shapes of crystal surfaces, in preparation.
- [10] R. Kenyon, A. Okounkov, S. Sheffield Dimers and amoebae, math-ph/0311005, to appear, *Ann. Math.*
- [11] R. Kenyon, J. Propp, D. Wilson, Trees and matchings. *Electr. J. Combin.* **7** (2000), research paper 25.
- [12] R. Kenyon, S. Sheffield, Dimers, tilings and trees, preprint. math.CO/0310195.
- [13] L. Lovasz, M. Plummer, Matching Theory, North-Holland Mathematics Studies, **121** Annals of Discrete Mathematics **29** North-Holland Publishing Co., Amsterdam (1986).
- [14] S. Sheffield, Gaussian free fields for mathematicians, preprint, math.PR/0312099.
- [15] S. Sheffield, thesis, Stanford University, 2002.